The interplay of wind and uplift facilitates over-water flight in facultative soaring birds

Elham Nourani, Gil Bohrer, Paolo Becciu, Richard O. Bierregaard, Olivier Duriez, Jordi Figuerola, Laura Gangoso, Sinos Giokas, Hiroyoshi Higuchi, Christina Kassara, Olga Kulikova, Nicolas Lecomte, Flavio Monti, Ivan Pokrovsky, Andrea Sforzi, Jean-François Therrien, Nikos Tsiopelas, Wouter M.G. Vansteelant, Duarte S. Viana, Noriyuki M. Yamaguchi, Martin Wikelski, and Kamran Safi

Proceedings of the Royal Society B: Biological Sciences
DOI: 10.1098/rspb.2021.1603

Abstract

Flying over the open sea is energetically costly for terrestrial birds. Despite this, over-water journeys of many birds, sometimes hundreds of kilometers long, are uncovered by bio-logging technology. To understand how these birds afford their flights over the open sea, we investigated the role of atmospheric conditions, specifically wind and uplift, in subsidizing over-water flight at the global scale. We first established that ΔT, the temperature difference between sea surface and air, is a meaningful proxy for uplift over water. Using this proxy, we showed that the spatio-temporal patterns of sea-crossing in terrestrial migratory birds is associated with favorable uplift conditions. We then analyzed route selection over the open sea for five facultative soaring species, representing all major migratory flyways. The birds maximized wind support when selecting their sea-crossing routes and selected higher uplift when suitable wind support was available. They also preferred routes with low long-term uncertainty in wind conditions. Our findings suggest that, in addition to wind, uplift may play a key role in the energy seascape for bird migration that in turn determines strategies and associated costs for birds crossing ecological barriers such as the open sea.

Supplementary material

Supplementary Figure 1

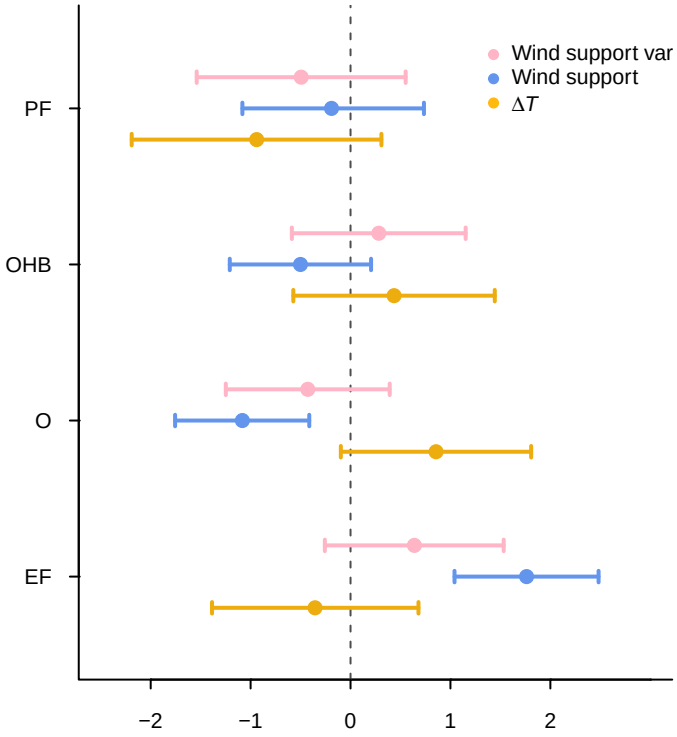

Figure S1: Species-specific variation in route selection. Posterior means and 95 % credible intervals are shown for the species-level random effects of the best INLA model.

Supplementary Figure 2

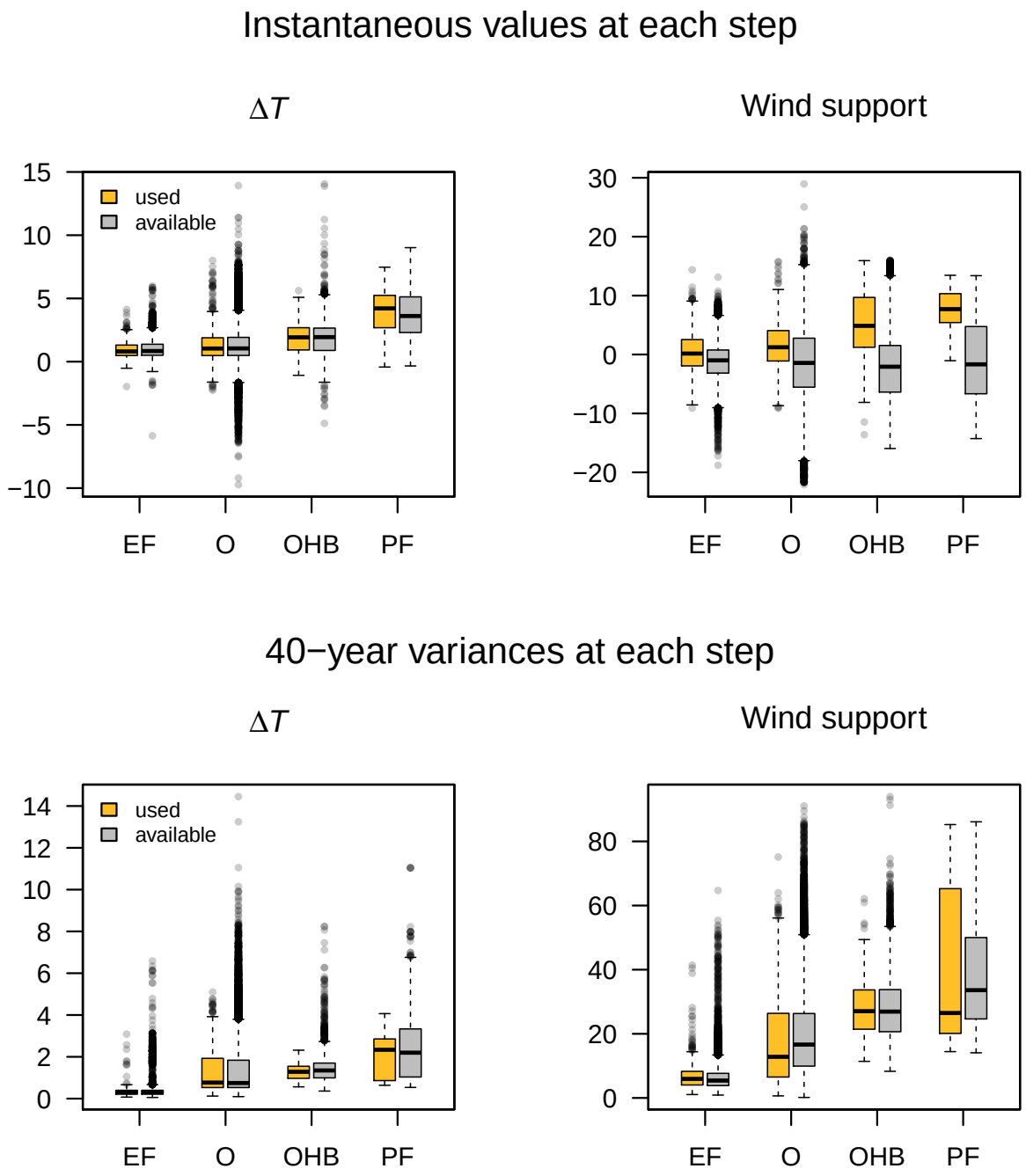

Figure S2: Distribution of values over the used and available steps. These were used for building the step-selection functions. The top row shows the instantaneous values and the bottom row the long-term variances. In the top row, it can be seen that wind support has more variability than ΔT and higher values of wind support are selected by the birds.

Supplementary Figure 3

Figure S3: Bio-logging data for sea-crossing tracks annotated with wind support and ΔT. Data is pooled for sea-crossing segments during autumn migration of the Oriental honey buzzard *Pernis ptilorhynchus* and the grey-faced buzzard *Butastur indicus* in the East Asian flyways, the osprey *Pandion haliaetus* and the peregrine falcon *Falco peregrinus*, in both the African-Eurasian and the American flyways, and the Eleonora's falcon *Falco eleonorae* in the African-Eurasian flyway. For samples of complete tracks, see Fig. **??**.

Supplementary Figure 4

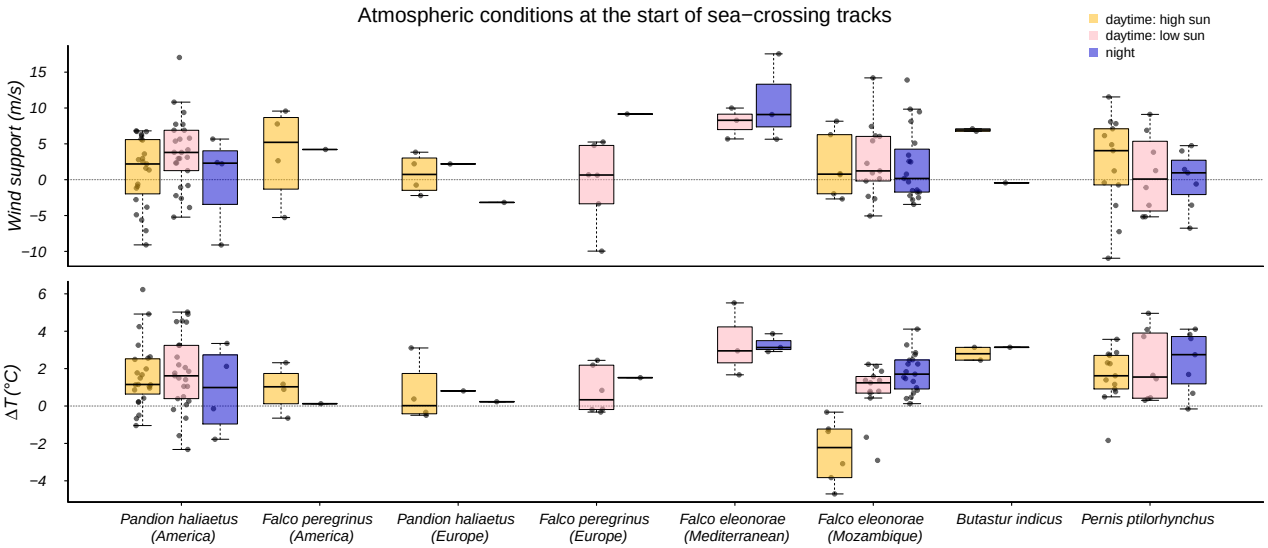

Figure S4: Wind support and ΔT values at the start of each sea-crossing track, grouped by time of day. Most species initiated sea-crossing with positive ΔT and tailwind. An overview of wind support and ΔT along the sea-crossing tracks is presented in Fig. S3.

Supplementary Table 1

Table S1: Summary of bio-logging data used in the step-selection function analysis. The number of individuals and migratory tracks correspond to the data that were retained after filtering the raw data set (see methods). The corresponding Movebank study names are shown in the footnotes.

Species	Tagging_location	Device	Years	Individuals	Tracks
Eleonora's falcon	Greece	GPS	2015	3	3
Eleonora's falcon	Spain	GPS	2012-2018	10	19
Oriental honey buzzard	Japan	GPS	2017-2019	8	17
Osprey [a]	South Europe	GPS	2013-2019	4	4
Osprey [b]	North America	GPS	2010-2019	10	15
Peregrine falcon [c]	North Europe	GPS	2018-2020	4	5
Peregrine falcon [c]	North America	GPS	2016	3	3
Totals				42	66

[a] Osprey in Mediterranean (Corsica, Italy, Balearics)

[b] Osprey Bierregaard North and South America

[c] LifeTrack Peregrine falcon

Supplementary Table 2

Table S2: Results of regional GAMMs built using forty years of global temperature data. These models were used for constructing energy seascapes (Fig. 2).

East Asia

A. parametric coefficients	Estimate	Std. Error	t-value	p-value
(Intercept)	-0.5051	0.0092	-54.9250	< 0.0001
sun_elev_flow	2.1566	0.0114	189.5042	< 0.0001
sun_elev_fnight	2.3400	0.0103	227.6074	< 0.0001
B. smooth terms	edf	Ref.df	F-value	p-value
s(lat,lon):sun_elev_fhigh	88.4643	88.4643	97.8487	< 0.0001
s(lat,lon):sun_elev_flow	91.2851	91.2851	196.2278	< 0.0001
s(lat,lon):sun_elev_fnight	92.7295	92.7295	190.2838	< 0.0001
s(yday):sun_elev_fhigh	7.6664	8.0000	231.6346	< 0.0001
s(yday):sun_elev_flow	7.7456	8.0000	228.6311	< 0.0001
s(yday):sun_elev_fnight	7.7940	8.0000	471.8103	< 0.0001
s(year)	0.0000	1.0000	0.0018	< 0.0001

The Americas

A. parametric coefficients	Estimate	Std. Error	t-value	p-value
(Intercept)	0.0296	0.0108	2.7394	0.0062
sun_elev_flow	1.3794	0.0129	106.6076	< 0.0001
sun_elev_fnight	1.6410	0.0126	130.5864	< 0.0001
B. smooth terms	edf	Ref.df	F-value	p-value
s(lat,lon):sun_elev_fhigh	90.0437	90.0437	169.5629	< 0.0001
s(lat,lon):sun_elev_flow	94.5179	94.5179	141.5539	< 0.0001
s(lat,lon):sun_elev_fnight	95.7668	95.7668	197.9859	< 0.0001
s(yday):sun_elev_fhigh	7.4179	8.0000	326.2731	< 0.0001
s(yday):sun_elev_flow	7.4498	8.0000	787.2890	< 0.0001
s(yday):sun_elev_fnight	7.2856	8.0000	524.7097	< 0.0001
s(year)	0.0000	1.0000	0.0000	0.8275

Indian Ocean

A. parametric coefficients	Estimate	Std. Error	t-value	p-value
(Intercept)	-0.1858	0.0051	-36.2476	< 0.0001
sun_elev_flow	0.0578	0.0065	8.8270	< 0.0001
sun_elev_fnight	1.2402	0.0057	216.8062	< 0.0001
B. smooth terms	edf	Ref.df	F-value	p-value
s(lat,lon):sun_elev_fhigh	94.7248	94.7248	231.4795	< 0.0001
s(lat,lon):sun_elev_flow	96.0323	96.0323	170.5800	< 0.0001
s(lat,lon):sun_elev_fnight	95.7945	95.7945	151.6102	< 0.0001
s(yday):sun_elev_fhigh	7.9279	8.0000	1455.4752	< 0.0001
s(yday):sun_elev_flow	7.9261	8.0000	1537.6625	< 0.0001
s(yday):sun_elev_fnight	7.9736	8.0000	5190.4193	< 0.0001
s(year)	0.0000	1.0000	0.0000	0.8801

Europe

A. parametric coefficients	Estimate	Std. Error	t-value	p-value
(Intercept)	-1.3977	0.0943	-14.8277	< 0.0001
sun_elev_flow	2.3936	0.0953	25.1193	< 0.0001
sun_elev_fnight	3.4697	0.0955	36.3168	< 0.0001
B. smooth terms	edf	Ref.df	F-value	p-value
s(lat,lon):sun_elev_fhigh	2.0000	2.0000	56.3685	< 0.0001
s(lat,lon):sun_elev_flow	75.6502	75.6502	14.5510	< 0.0001
s(lat,lon):sun_elev_fnight	82.6352	82.6352	40.0598	< 0.0001
s(yday):sun_elev_fhigh	6.0995	8.0000	210.8682	< 0.0001
s(yday):sun_elev_flow	7.8303	8.0000	1434.8943	< 0.0001
s(yday):sun_elev_fnight	7.6710	8.0000	1046.5831	< 0.0001
s(year)	0.0000	1.0000	0.0000	0.0634

Mozambique Channel

A. parametric coefficients	Estimate	Std. Error	t-value	p-value
(Intercept)	0.1469	0.0279	5.2605	< 0.0001
sun_elev_flow	0.2450	0.0334	7.3248	< 0.0001
sun_elev_fnight	1.7059	0.0280	61.0334	< 0.0001
B. smooth terms	**edf**	**Ref.df**	**F-value**	**p-value**
s(lat,lon):sun_elev_fhigh	89.1660	89.1660	30.6120	< 0.0001
s(lat,lon):sun_elev_flow	71.4595	71.4595	165.7619	< 0.0001
s(lat,lon):sun_elev_fnight	95.5807	95.5807	83.2314	< 0.0001
s(yday):sun_elev_fhigh	6.5492	8.0000	362.2948	< 0.0001
s(yday):sun_elev_flow	7.5523	8.0000	299.7936	< 0.0001
s(yday):sun_elev_fnight	7.5972	8.0000	608.8270	< 0.0001
s(year)	0.0001	1.0000	0.0002	0.0780